Optimization of Slitlike Carbon Nanopores for Storage of hythane Fuel at Ambient Temperatures

Piotr Kowalczyk*

Department III, Soft Condensed Matter, Institute of Physical Chemistry, Polish Academy of Science, Kasprzaka Street 44/52, 01-224 Warsaw, Poland

Suresh K. Bhatia

Division of Chemical Engineering, The University of Queensland, St. Lucia, Qld 4072, Australia

Received: July 13, 2006; In Final Form: September 16, 2006

Carbons with slitlike pores can serve as effective host materials for storage of hythane fuel, a bridge between the petrol combustion and hydrogen fuel cells. We have used grand canonical Monte Carlo simulation for the modeling of the hydrogen and methane mixture storage at 293 K and pressure of methane and hydrogen mixture up to 2 MPa. We have found that these pores serve as efficient vessels for the storage of hythane fuel near ambient temperatures and low pressures. We find that, for carbons having optimized slitlike pores of size $H \cong 7$ Å (pore width that can accommodate one adsorbed methane layer), and bulk hydrogen mole fraction ≥ 0.9, the volumetric stored energy exceeds the 2010 target of 5.4 MJ dm^{-3} established by the U.S. FreedomCAR Partnership. At the same condition, the content of hydrogen in slitlike carbon pores is ≅7% by energy. Thus, we have obtained the composition corresponding to hythane fuel in carbon nanospaces with greatly enhanced volumetric energy in comparison to the traditional compression method. We proposed the simple system with added extra container filled with pure free/adsorbed methane for adjusting the composition of the desorbed mixture as needed during delivery. Our simulation results indicate that light slit pore carbon nanomaterials with optimized parameters are suitable filling vessels for storage of hythane fuel. The proposed simple system consisting of main vessel with physisorbed hythane fuel, and an extra container filled with pure free/adsorbed methane will be particularly suitable for combustion of hythane fuel in buses and passenger cars near ambient temperatures and low pressures.

Introduction

The recent interest in the hydrogen economy has coincided with the rapid development of fuel cells, creating much interest worldwide in the automotive and energy industries. The introduction of hydrogen as a fuel in the transportation sector has, however, been delayed by the absence of a safe and economical means of on-board storage. Among the conventional options for storage, compressed gas suffers from concerns about safety, while liquefaction is not cost competitive. Several new options are now being widely investigated, such as storage by hydrides,[1,2] by clathrate hydrates,[3] or by nanoporous adsorbents.[4,5] However, all of these options have their drawbacks and are still not viable. For example, hydrides suffer from the problem of high-desorption temperatures,[1,2] while physisorption in nanoporous adsorbents such as carbon can only meet required storage densities and deliveries at low temperatures.[6] As a result of these difficulties, a viable hydrogen storage technology is yet to emerge, and introduction of hydrogen as a transportation fuel is still only a possibility for the future.

Given the above difficulties in harnessing hydrogen as a transportation fuel, it has become necessary to examine alternate fuels for the near term. Methanol is one such possibility, but it is toxic and also corrosive to fuel cell electrodes. In addition, CO_2 released during its direct combustion in fuel cells is a poison that reduces process efficiency.[7] Natural gas is another option, already in some use, but it is predominantly comprised of methane, a fairly stable molecule with much lower flammability as well as flame speed relative to hydrogen.[8] This limits its combustion efficiency, not only in the engine, but also in the subsequent catalytic converter,[8] leading to undesirable hydrocarbon emissions.

To overcome the above drawbacks of natural gas, a new fuel, hythane, has been proposed which is a blend comprising 20% H_2 and 80% CH_4 by volume.[8,9] In this proportion, hydrogen contributes only about 7% of the heat of combustion of hythane, but because of its higher flammability as well as 8 times larger flame speed, it acts as a catalyst which accelerates methane combustion within the engine. Further, its presence also leads to lowering of harmful emissions of nitrogen oxides CO_2 and low-volatile organics.[8,9] Thus, it would appear that hythane is a viable interim fuel for the near term, as we progress toward a viable hydrogen economy.

As with the case of hydrogen, on-board storage of hythane is an issue that requires attention. While compressed hythane is less hazardous than compressed hydrogen, an alternative such as adsorptive storage would improve its viability for widespread use, particularly for passenger automobiles. In the current paper, we used grand canonical Monte Carlo (GCMC) simulation to investigate carbons with slitlike nanopores as potential host materials for efficient storage of hythane fuel at 293 K and pressure of hydrogen and methane mixture up to 2 MPa. Storage

* To whom correspondence should be addressed. Tel: 81−43−290−2779; fax: 81−43−290−2788; e-mail: kowal@kora.ichf.edu.pl.

10.1021/jp064428h CCC: $33.50
Published on Web 10/31/2006

in this type of carbonaceous material (i.e., activated carbons, activated carbon fibers, etc.) has several advantages. First, the hydrogen and methane molecules are physisorbed so simple manipulation of temperature or pressure can be used for controlled release of the stored fuel. Second, these carbonaceous materials are lightweight, cheap, chemically inert, thermally stable, and environmentally friendly. Indeed, common carbonaceous materials such as those mentioned above have been widely used in industry for purification and separation as well as other processes.[10−12]

Simulation Methods

a. Fluid−Fluid Interaction Potential. Similar to Cracknell and Nicholson[13] and Kowalczyk et al.,[14] we modeled the methane−methane interactions via the effective truncated one-center Lennard-Jones potential (i.e., we treated the methane as a quasi-spherical molecule)

$$V_{\mathrm{ff}} = 4\epsilon_{\mathrm{ff}}\left[\left(\frac{\sigma_{\mathrm{ff}}}{r}\right)^{12} - \left(\frac{\sigma_{\mathrm{ff}}}{r}\right)^{6}\right]\Theta(r_{\mathrm{cut}} - r) \qquad (1)$$

Here, r is the distance between two interacting fluid molecules, σ_{ff} denotes Lennard-Jones collision diameter, ϵ_{ff} is the Lennard-Jones well-depth, $r_{\mathrm{cut}} = 5\sigma_{\mathrm{ff}}$ is the cutoff distance, and Θ denotes Heaviside function. The Lennard-Jones parameters for methane interactions, $\sigma_{\mathrm{ff}} = 3.81$ Å and $\epsilon_{\mathrm{ff}}/k_{\mathrm{b}} = 148.12$ K (k_{b} denotes Boltzmann's constant), were taken from previous studies.[13,14] This simple one-center Lennard-Jones spherical potential with parameters given above has been shown to correctly describe the experimental equation of state near ambient temperatures.[14]

Following Sese,[15,16] Kowalczyk et al.,[17] Levesque et al.,[18] and Tanaka and co-workers,[19,20] we assumed that the hydrogen molecules interact via the quadratic Feynman−Hibbs quantum effective potential

$$V_{\mathrm{ff}}(r) = V_{\mathrm{LJ}}(r) + \frac{\beta\hbar^2}{24\mu_m}\left[\frac{d^2}{dr^2}V_{\mathrm{LJ}}(r) + \frac{2}{r}\frac{d}{dr}V_{\mathrm{LJ}}(r)\right] \qquad (2)$$

where the classical potential is represented by a one-center Lennard-Jones spherical potential, similar to that in eq 1. Here, $\beta = (k_{\mathrm{b}}T)^{-1}$, $\hbar = h/2\pi$, $\mu_{\mathrm{m}} = m/2$ is the reduced mass of a pair of interacting hydrogen molecules, and h denotes Planck's constant. For hydrogen, we used the classical parameters[17−20] $\sigma_{\mathrm{ff}} = 2.958$ Å and $\epsilon_{\mathrm{ff}}/k_{\mathrm{b}} = 36.7$ K. The second term in eq 2 accounts for quantum corrections to the statistical properties generated by the classical Lennard-Jones potential. Near ambient temperature, the quantum corrections in the bulk hydrogen can be neglected.[17] The approximation of the diatomic hydrogen molecule by an effective Lennard-Jones sphere is justified by the high temperature and low-density region investigated in the current study. In a previous study, we showed that the effective second-order Feynman−Hibbs or simple Lennard-Jones potential with parameters given above correctly describes the experimental bulk equation of state.[17]

Hydrogen−methane interactions were modeled according to eqs 1 and 2 with μ representing the reduced quantum mass of the interacting molecules. Hydrogen/methane Lennard-Jones parameters were obtained from the commonly used Lorentz−Berthelot mixing rules.[12]

b. Solid−Fluid Interaction Potential. The total methane−carbon interaction potential is a sum of those generated from

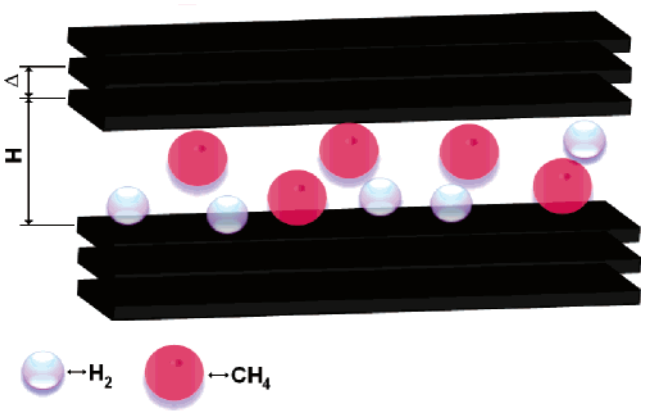

Figure 1. Molecular model of hydrogen and methane mixture adsorption in slitlike carbon pore.

infinite planes comprising the walls of the slitlike pore (see Figure 1)[21−23]

$$V^{\mathrm{sf}}{}_{\mathrm{T}}(Z) = \sum_{j=0}^{M-1} V^{sf}{}_{10-4}(H - Z + j\cdot\Delta) + \sum_{j=0}^{M-1} V^{sf}_{10-4}(Z + j\cdot\Delta) \qquad (3)$$

Here, $M - 1$ denotes the number of graphite planes comprising the pore wall (here, $M = 4$) and H denotes slit width (cf. Figure 1). The distance between graphic planes is taken as that for graphite ($\Delta = 3.35$ Å[24]). The potential between a methane molecule and a single infinite plane of structureless graphite is modeled by the Steele 10−4 potential[24,25]

$$V^{sf}_{10-4}(Z) = 4\epsilon_{\mathrm{sf}}\pi\rho_{\mathrm{s}}\sigma^2{}_{\mathrm{sf}}\left[\frac{1}{5}\left(\frac{\sigma_{\mathrm{sf}}}{Z}\right)^{10} - \frac{1}{2}\left(\frac{\sigma_{\mathrm{sf}}}{Z}\right)^{4}\right] \qquad (4)$$

where $\rho_{\mathrm{s}} = 38.2$ nm^{-2} is the surface density of carbon atoms, σ_{sf} and ϵ_{sf} denote Lennard-Jones solid−fluid collision diameter and well-depth, respectively, and Z is the distance of the methane molecule from the plane. The parameters of the solid−fluid potential were calculated from the Lorentz−Berthelot mixing rule.[12,25] For carbon, we adapted the following values of parameters: $\sigma_{\mathrm{ss}} = 3.4$ Å and $\epsilon_{\mathrm{ss}}/k_{\mathrm{b}} = 28$ K.[24] The adopted rigid model of infinitely long slitlike carbon pore is realistic for materials whose pore walls consist of three and more graphite planes (i.e., high-graphitized soft-activated carbons, homogeneous activated carbon fibers). For these types of carbonaceous materials, the deformation of the pore walls during adsorption−desorption of weakly interacting hydrogen or methane can be neglected. On the other hand, the rigid model of the basic carbon unit may be a crude approximation for activated carbons whose thick pore walls are composed of single graphite planes. For these kinds of carbonaceous nanomaterials, the slitlike pore width is "ill-defined" because of deformation and bending of the pore walls during the adsorption−desorption of adsorbates.

In confinement, quantum effects are enhanced in comparison with the bulk phase because of the very large potential gradients which exist within objects of nanoscale dimensions and, as a consequence, the motion of quantum molecules is restricted in some directions. For very small carbon nanopores, the quantum effects cannot be neglected even at 293 K. For this reason, the total hydrogen−carbon interaction potential is corrected for quantum effects according to the second-order Feynman−Hibbs effective potential,[26] in a manner similar to that in eq 2 for the fluid−fluid potential. As for methane, we used the Lorentz−Berthelot mixing rule for estimation of hydrogen−carbon Lennard-Jones parameters.[12,25]

c. Simulation Details. In the present work, we performed the simulation of hydrogen and methane mixture adsorption at 293 K, for bulk mixture pressure up to 2 MPa. We assumed that the mixture is ideal under this condition and that Dalton's law is obeyed, that is, the mixture pressure is the sum of the partial pressures of the individual components.[12]

In the simulation of hydrogen and methane mixture in the idealized infinitely long slitlike carbon pores, we used a grand canonical ensemble (i.e., fixed system volume, temperature, and chemical potential of the bulk fluid mixture).[27,28] For perturbation of the configuration in GCMC, we select hydrogen or methane molecules with equal probability. Equal probabilities are used for trial moves, creation, and destruction of the selected molecule, and the acceptance decision follows the Metropolis sampling scheme.[27,28] We calculated the excess part of the chemical potential of hydrogen and methane in the canonical ensemble according to Widom's particle insertion method and the corresponding bulk pressure of hydrogen from the virial theorem.[29] As usual, we added the tail corrections for the energy and pressure after the simulation has been completed.[27,28] A cubic simulation box of size $10\sigma_{ff} \times 10\sigma_{ff} \times H$ ($\sigma_{ff} = 3.81$ Å) with periodic boundary conditions in x and y directions was used, with the minimum image convention used for computation of molecular interactions.[27,28] The grand canonical ensemble simulations utilized 1×10^8configurations, of which the first 6×10^7 were discarded to guarantee equilibration. The stability of the results was confirmed by additional longer runs of 1.6×10^8 configurations, with the equilibrium composition of hydrogen and methane mixture in pores fully reproducible.

d. Storage Efficiency. GCMC simulation allows for a precise determination of the total uptake of methane and hydrogen mixture in pore at thermodynamic equilibrium because the geometry of the adsorbent is specified. On the basis of the absolute value of adsorption, the total stored volumetric energy was calculated following the expression

$$\Omega = \Gamma_{H_2} \cdot (-\Delta H_{H_2}) + \Gamma_{CH_4} \cdot (-\Delta H_{CH_4}) \qquad (5)$$

Here, ΔH_{H_2} and ΔH_{CH_4} denote the heat of hydrogen and methane combustion (i.e., heat of reaction per mole equates to the difference in enthalpy of the products and the reactants), respectively. Following Dell and Rand,[30] the methane heat of combustion is -55.6 MJ per kg methane. For hydrogen, the heat of combustion equates to the heat of formation of the product water,[30] that is, -285.83 kJ per mol water (-141.789 MJ per kg hydrogen). For industrial application, we are interested in total volumetric energy stored during adsorption of molecules in slitlike carbon pores of various sizes. Promising porous materials should accommodate a large number of molecules in comparison to the bulk phase (i.e., compressed fluid).

On the other hand, the content of adsorbed hydrogen in total stored volumetric energy is critical for combustion properties of hythane fuel.[8,9] High content of hydrogen in hythane fuel causes the increasing of emission of harmful gases because of high temperature of combustion. Low content of hydrogen in hythane fuel does not improve the methane properties (ignition time, flammability range, flame speed, etc.) and does not reduce air pollution. According to experimental reports, the content of hydrogen in hythane fuel should be $\cong 6-7\%$ by energy.[8,9] GCMC simulation allows for a precise determination of the content of hydrogen by energy in adsorbed hydrogen and methane mixture

$$\Psi\,[\%] = 100 \cdot \frac{\Gamma_{H_2} \cdot (-\Delta H_{H_2})}{\Omega} \qquad (6)$$

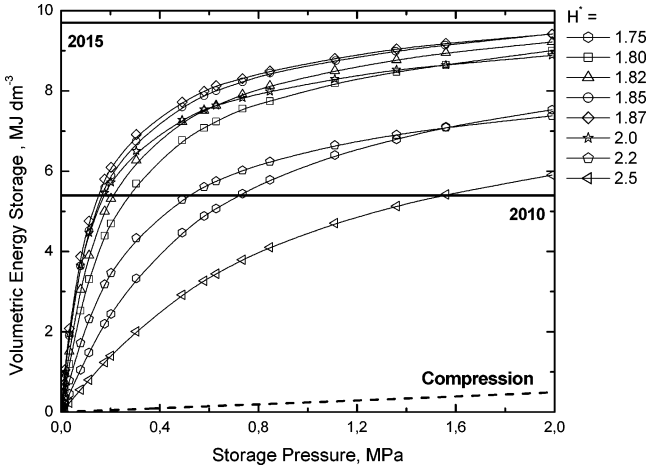

Figure 2. Pressure variation of stored volumetric energy of equimolar mixture of hydrogen and methane in various slit pore sizes at 293 K. The reduced width of the pore is given by $H^* = H/\sigma_{ff}$, $\sigma_{ff} = 3.81$ Å. Solid lines correspond to targets established by the U.S. FreedomCAR Partnership: 5.4 MJ.dm^{-3} by 2010 and 9.7 MJ.dm^{-3} by 2015. Dashed line corresponds to the volumetric energy of the compressed equimolar mixture of hydrogen and methane.

While important from a storage efficiency viewpoint, the quantities Ω and Ψ are not directly accessible by experiment as the absolute amount adsorbed, Γ_{H_2}, cannot be directly measured. The quantity that is experimentally measurable is the excess of adsorption, which is the amount of adsorbate in excess of that of bulk fluid at the same temperature and pressure and in the same available volume. However, computer simulations such as those conducted here permit these quantities to be reliably predicted. Good accuracy of simulation in predicting adsorption in slit pore carbons, in agreement with experiment, has been documented.[31]

Result and Discussion

We consider the storage of the equimolar mixture of hydrogen and methane in slitlike carbon pores of various sizes. Our simulations indicate that the total stored volumetric energy (i.e., sum of the adsorbed methane and hydrogen combustion energies) greatly exceed that obtained from simple compression method, as seen in Figure 2. Moreover, carbons with slitlike pores in the size range $H^* \cong 1.8-2.0$ exceed the 2010 target established by U.S. FreedomCAR Partnership[30] at 293 K and low pressures of the mixture. Unfortunately, while these sizes would appear optimal in terms of volumetric energy storage efficiency, as we can find from Figure 3, the contribution of hydrogen in the total stored energy for these pore sizes is very low ($\cong 2-3\%$) compared to hythane fuel.[8,9] Increasing pore size of the carbon increases the amount of adsorbed hydrogen; however, the total stored energy quickly goes down. The observed phenomena can be simply explained. The main content of the total stored volumetric energy comes from the adsorbed methane. As one can see from selected equilibrium snapshots displayed in Figure 4, methane is strongly adsorbed in slitlike carbon pores of the above optimal sizes at 293 K and low pressures of the mixture. The size of this optimum slitlike carbon pore can accommodate one adsorbed layer of methane. In this

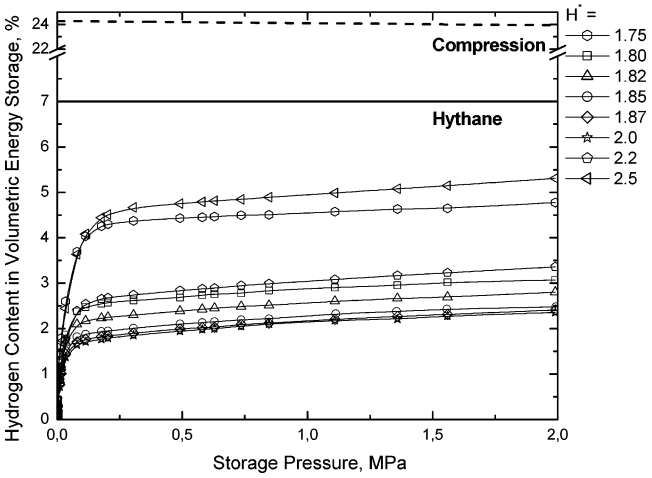

Figure 3. The content of hydrogen in stored volumetric energy of equilateral mixture of hydrogen and methane in selected slitlike carbon pores at 293 K. The reduced width of the pore is given by $H^* = H/\sigma_{ff}$, $\sigma_{ff} = 3.81$ Å. Solid line corresponds to the contribution of hydrogen in hythane fuel (≅7% by energy). Dashed line corresponds to the contribution of hydrogen to the volumetric energy of the compressed equimolar mixture of hydrogen and methane.

"perfect slitlike carbon pore", methane is efficiently packed and compressed in nanospaces. At the same time, hydrogen is weakly adsorbed from the equimolar mixture of methane and hydrogen because of its relatively weak solid−fluid and fluid−fluid interaction energy near ambient temperature.[17] An increase in hydrogen content in wider as well as narrower pores occurs, as seen in Figure 3. Reduction of pore width causes "sieving effect" of hydrogen. In other words, hydrogen is efficiently adsorbed in the smallest pore sizes because of enhanced solid−fluid interactions, whereas methane has no access to these pores because of simple geometric constraints (i.e., steric forces). Another important case is when the width of the slitlike carbon pore can accommodate more than one adsorbed layer of methane. The first observation is a decrease of the total stored volumetric energy, accompanied by increasing contribution of hydrogen in the total stored volumetric energy. This behavior is consistent with previous stimulations of Lennard-Jones mixtures in confinement.[12−14] First, the methane−carbon interaction is reduced, which leads to the reduced densification of supercritical fluids in confinement. Second, because of imperfect placing of methane molecules in slitlike carbon pores, the densification of hydrogen is energetically favorable.

To better understand the competition between hydrogen and methane adsorption, we have computed the total isosteric heat of adsorption of the equimolar hydrogen and methane mixture, as displayed in Figure 5. As is the case for pure methane adsorption in similar conditions, the highest isosteric heat of adsorption (≅20−25 kJ mol^{-1}) is observed during loading of pores lying in the optimal pore size range for storage of energy, that is, $H^* \cong 1.8-2.0$.[6,14] Consequently, we attribute the large heat release during adsorption of hydrogen and methane mixture to the strong binding of methane by the carbon surfaces comprising the slit pore. Increasing or decreasing of the slit carbon pore size drastically reduces the isosteric heat of adsorption since hydrogen is weakly interacting with carbon surfaces near ambient temperature.[6,17] Consequently, for efficient storage of hythane fuel, it is necessary to adjust the bulk composition of hydrogen and methane mixture near ambient temperatures to obtain both high total volumetric stored energy and proper content of hydrogen in the adsorbed phase. Thus, it is necessary to replace some methane molecules by hydrogen in the adsorbed phase.

We now focus our attention to the case of mole fraction of hydrogen in the bulk mixture of 0.9, depicted in Figures 6 and 7. The first observation is that the total stored volumetric energy is reduced for the higher mole fraction of hydrogen in the bulk hydrogen and methane mixture. However, the total stored volumetric energy still exceeds the 2010 target established by the U.S. FreedomCAR Partnership[30] for 293 K and low pressures (cf. Figure 6). At the same time, the contribution of hydrogen in the total stored volumetric energy increases up to 6−7% (cf. Figure 7) in the optimal slit pores lying in the range $H^* \cong 1.8-2.0$. Upon careful analysis of the selected equilibrium snapshots displayed in Figure 8, we conclude that methane is preferentially adsorbed in the optimal pore sizes even for molar fraction of hydrogen ≥0.9 in the bulk phase mixture. However, the contribution of hydrogen to the total stored volumetric energy is optimized for the hythane fuel composition.[8,9] On the basis of these results, it is clear that the hythane fuel composition is attained in slitlike carbon pores near ambient temperatures and low pressures. Contrary to simple classical compression of the bulk hythane fuel, our stored hydrogen and methane adsorbed phase of the hythane fuel composition is characterized by much larger volumetric energy because of efficient densification of hydrogen and methane mixture in carbon nanospaces (cf. Figure 6). It is not surprising that the total isosteric heat of hydrogen and methane adsorption from hydrogen-rich bulk phase mixture is reduced in comparison to the equimolar bulk mixture (cf. Figure 9). This fact is attributed to the higher content of hydrogen in the adsorbed phase.

Up till now, we have been concentrated on the equilibrium composition of bulk/adsorbed hydrogen and methane mixture. The remaining problem of great importance is delivery of the energy. Even assuming the fast desorption of both methane and hydrogen, so that equilibrium is always maintained as the pressure reduces with consumption, at first when the container pressure is 2 MPa more hydrogen will be desorbed. It results from the high mole fraction of hydrogen in the bulk-phase mixture. We expect that after some period of delivery time the hydrodynamic flow should on average be characterized by the composition close to adsorbed hythane fuel composition. Finally, when the fuel supply is near exhaustion, more methane will be desorbed. One possible way to adjust the composition of desorbed fluid to that of the hythane fuel is to use a second container with pure methane, with the mixture container charged with higher than 7% of hydrogen by energy, if possible, in the adsorbate. Then, on delivery, hydrogen energy from the mixture cylinder is high (i.e., for some time after start of desorption), and the gas is supplemented with methane from the pure gas container. Desorption of mixture is stopped when the hydrogen content by energy falls below 7% in the mixture container product. This container is then charged again. The second container could also be adsorbed methane to minimize the size of the extra container. The proposed variant of the hythane fuel delivery can be justified by the properties of the supercritical fluid mixture. First, hydrogen mixes perfectly with methane in supercritical state. Second, supercritical fluids rapidly diffuse to occupy the entire volume of the stored system. Finally, the properties of the supercritical mixture can be easily tuned by the temperature or pressure. The experimental problem to solve is the aging of the carbon bed in terms of loading/releasing cycles.

In summary, our computation study brings new light into the potential hythane fuel storage in slitlike carbon, despite the

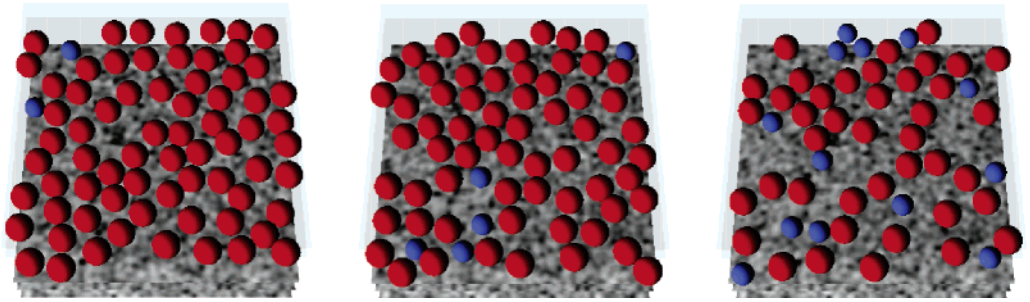

Figure 4. Equilibrium snapshot of hydrogen and methane mixture for different molar ratio of hydrogen and methane in the bulk phase at 293 K and total pressure of hydrogen and methane mixture of 2 MPa. From left to right: $y_{H_2} = 0.2$; $y_{H_2} = 0.5$; $y_{H2} = 0.95$. The reduced pore width is $H^* = H/\sigma_{ff} = 1.85$, $\sigma_{ff} = 3.81$ Å.

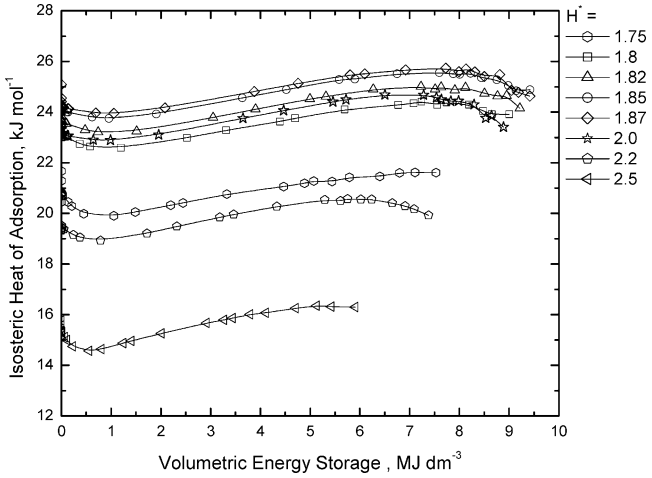

Figure 5. Isosteric heat of adsorption of an equimolar hydrogen and methane mixture at 293 K versus volumetric energy storage for selected slit pore sizes. The reduced width of the pore is given by $H^* = H/\sigma_{ff}$, $\sigma_{ff} = 3.81$ Å.

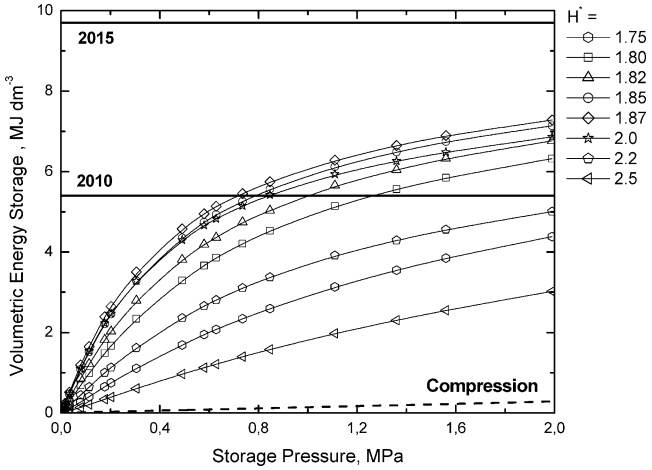

Figure 6. Variation of stored volumetric energy of mixture of hydrogen and methane with pressure, for bulk mole fraction of hydrogen of 0.9, in selected carbon slit pores at 293 K. The reduced width of the pore is given by $H^* = H/\sigma_{ff}$, $\sigma_{ff} = 3.81$ Å. Lines are as in Figure 2.

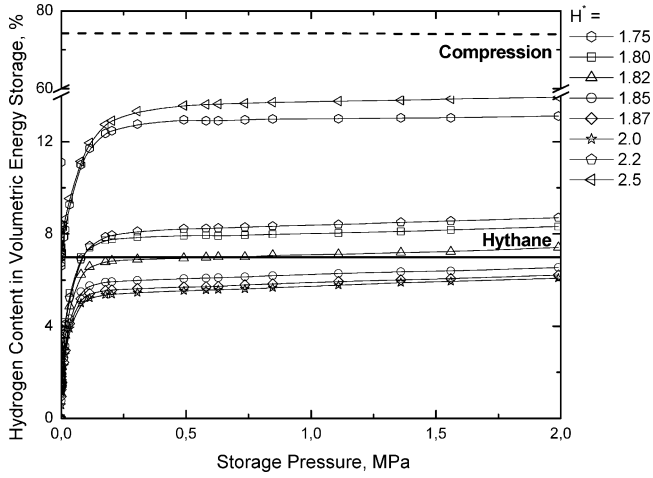

Figure 7. The contribution of hydrogen in stored volumetric energy of mixture of hydrogen and methane, for bulk mole fraction of hydrogen of 0.9, in selected carbon slit pores at 293 K. The reduced width of the pore is given by $H^* = H/\sigma_{ff}$, $\sigma_{ff} = 3.81$ Å. Lines are as in Figure 3.

idealized models adopted for the current studies. On the basis of the extensive simulations, we predict reduced optimal pore size for hythane storage of $H^* \cong 1.8-2.0$. Moreover, we showed that the proper mole fraction of hydrogen in the bulk hydrogen and methane mixture is critical for tuning of the adsorbed layer composition. Only mole fraction of hydrogen ≥ 0.9 in the bulk hydrogen and methane mixture guarantees proper content of hydrogen (i.e., hythane fuel composition) in the adsorbed phase at the condition of storage considered here. However, too much adsorbed hydrogen greatly reduces the total stored volumetric energy. Matranga et al.[32] reported that an optimal carbon slitlike pore width for methane storage is 1.14 nm (i.e., perfect pore that can accommodate two adsorbed layers of methane). For the case of hythane fuel, it is necessary to take into account the subtle interplay between the total sorted volumetric energy and the proper hydrogen content in the adsorbed phase. To keep the composition of hythane fuel (≈7% by energy or equivalent ≈20 vol %), more hydrogen molecules must be adsorbed in the larger pores. This excludes methane molecules from being the main component of the total stored energy in these pores. As a result, slitlike carbon pores of width 1.14 nm and greater are less attractive for hythane fuel storage in contrast to carbons having optimized slitlike pores of size $H \cong 7$Å (pore width that can accommodate one adsorbed methane layer). To adjust the composition of the desorbed fluid during hydrodynamic flow, we suggest a simple solution. The proposed additional system consists of a small container with pure methane and mixing container charged with higher than 7% of hydrogen by energy, if possible, in the adsorbate. When the high content of the hydrogen is detected in the desorbed fluid, the additional methane is automatically injected from the extra small container filled with pure bulk or adsorbed methane to ensure the hythane fuel composition. The production of carbons with narrowly sized slit pores seems to be a key factor for widespread application of these materials for storage of hythane fuel. Experimental investigations on the adsorption of hydrogen and methane

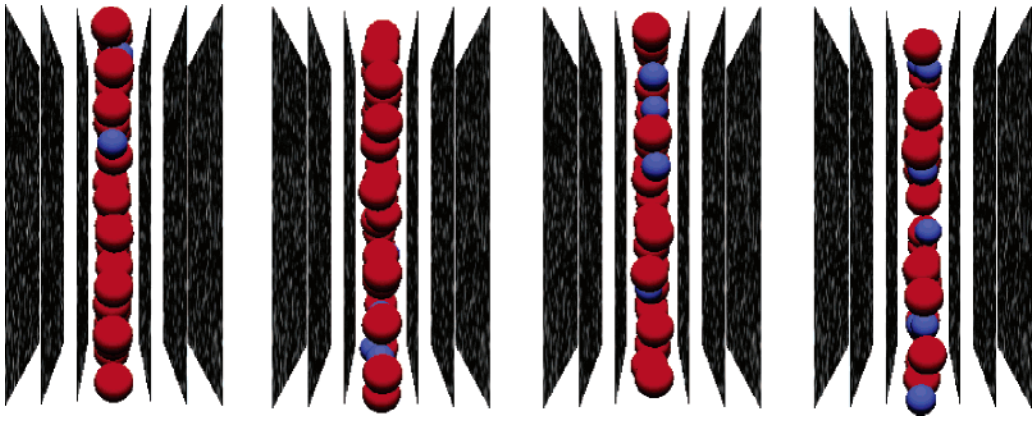

Figure 8. Equilibrium snapshot of hydrogen and methane mixture for different molar ratio of hydrogen and methane in the bulk phase (from left to right: $x_{H_2} = 0.2$, $x_{CH_4} = 0.8$; $x_{H_2} = 0.5$, $x_{CH_4} = 0.5$; $x_{H_2} = 0.9$, $x_{CH_4} = 0.1$; $x_{H_2} = 0.95$, $x_{CH_4} = 0.05$) at 293 K and total pressure of hydrogen and methane mixture 2 MPa. The reduced pore width is $H^* = H/\sigma_{ff} = 1.85$, $\sigma_{ff} = 3.81$ Å.

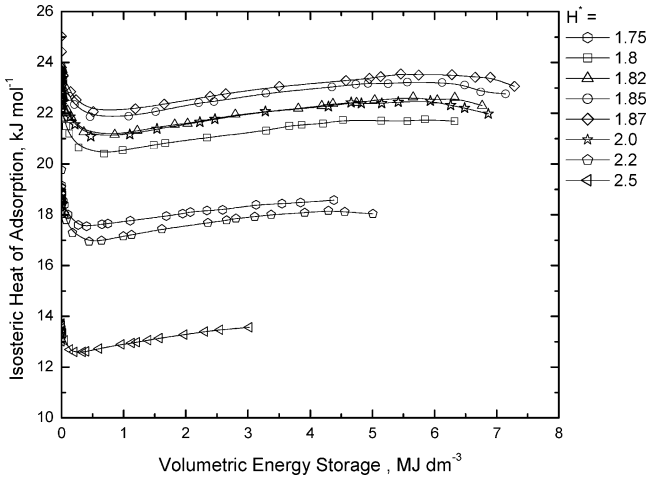

Figure 9. Correlation of isosteric heat of adsorption of hydrogen/methane mixture with volumetric energy storage, for bulk mole fraction of hydrogen of 0.9 at 293 K, for selected slit pore sizes. The reduced width of the pore is given by $H^* = H/\sigma_{ff}$, $\sigma_{ff} = 3.81$ Å.

mixture in activated carbon fibers and activated carbons are also needed for employing these as host materials on the industrial scale.

Conclusions

To our knowledge, this is the first computational study of hythane fuel storage in a nanoporous material. We have shown that slit pore carbons can serve as effective nanoporous host materials for storage of hythane fuel at 293 K and pressure of the methane and hydrogen mixture up to 2 MPa. For the optimum slit pore size (pore width that can accommodate exactly one adsorbed methane layer, $H \cong 7$Å, and bulk mole fraction of hydrogen ≥ 0.9), the volumetric stored energy exceeds the 2010 target of 5.4 MJ.dm^{-3} established by the U.S. Freedom-CAR Partnership. At the same condition, the contribution of hydrogen in slit carbon pores is $\cong$7% by energy, corresponding to hythane fuel. Moreover, the adsorbed and compressed methane and hydrogen molecules in carbon nanospaces greatly enhance the volumetric energy in comparison to traditional bulk compression. We proposed the simple system with added extra container filled with pure free/adsorbed methane for adjusting the composition of the desorbed mixture during hydrodynamics flow. Our simulation results indicate that light slit pore carbon nanomaterials with optimized parameters are suitable filling vessels for storage of hythane fuel. The proposed simple system consists of main vessel with physisorbed hythane fuel, and an extra container filled with pure free/adsorbed methane will be particularly suitable for combustion of hythane fuel in buses and passenger cars near ambient temperatures and low pressures.

Acknowledgment. P.K. gratefully acknowledges Professor A. Lasia (Sherbrooke University, Sherbrooke, Canada) for fruitful discussions considering the current paper.

References and Notes

(1) Hu, Y. H.; Yu, N. Y.; Ruckenstein, E. *Ind. Eng. Chem. Res.* **2004**, *43*, 4174.
(2) Alapati, S. V.; Johnson, J. K.; Sholl, D. S. *J. Phys. Chem. B* **2006**, *110*, 8769.
(3) Lee, H.; Lee, J.-W.; Kim, D. Y.; Park, J.; Seo, Y.-T.; Zeng, H.; Moudrakovski, I. L.; Ratcliffe, C. I.; Ripmeester, J. A. *Nature (London)* **2005**, *434*, 743.
(4) Schlapbach, L.; Züttel, A. *Nature (London)* **2005**, *414*, 353.
(5) Rowsell, J. L. C.; Millward, A. R.; Park, K. S.; Yaghi, O. M. *J. Am. Chem. Soc.* **2004**, *126*, 5666.
(6) Bhatia, S. K.; Myers, A. L. *Langmuir* **2006**, *22*, 1688.
(7) Hoogers, G. *Fuel Cell Technology Handbook*; CRC: Oxford, U.K., 2002.
(8) Green Car Congress website. www.greencarcongress.com.
(9) Hythane Company website. www.hythane.com.
(10) Harris, P. J. F. *Carbon Nanotubes and related structures. New Materials for the Twenty-first Century*; Cambridge University Press: Cambridge, U.K., 1999.
(11) Gregg, S. J.; Sing, K. S. W. *Adsorption, Surface Area and Porosity*; Academic Press: London, 1982.
(12) Gubbins, K. E.; Quirke, N. In *Molecular Simulation and Industrial Applications: Methods, Examples and Prospects;* Gubbins, K. E., Quirke, N. Eds.; Gordon and Breach Science Publishers: Amsterdam, 1996.
(13) Cracknell, R. F.; Nicholson, D. *Adsorption* **1995**, *1*, 7.
(14) Kowalczyk, P.; Tanaka, H.; Kaneko, K.; Terzyk, A. P.; Do, D. D. *Langmuir* **2005**, *21*, 5639.
(15) Sese, L. M. *Mol. Phys.* **1994**, *81*, 1297.
(16) Sese, L. M. *Chem. Phys. Lett.* **1997**, *266*, 130.
(17) Kowalczyk, P.; Tanaka, H.; Hołyst, R.; Kaneko, K.; Ohmori, T.; Miyamoto, J. *J. Phys. Chem. B* **2005**, *109*, 17174.
(18) Levesque, D.; Gicquel, A.; Darkrim, F. L.; Kayiran, S. B. *J. Phys. Condens. Matter* **2002**, *14*, 9285.
(19) Tanaka, H.; Fan, J.; Kanoh, H.; Yudasaka, M.; Iijima, S.; Kaneko, K. *Mol. Simul.* **2005**, *31*, 465.
(20) Tanaka, H.; Kanoh, H.; Yudasaka, M.; Iijima, S.; Kaneko, K. *J. Am. Chem. Soc.* **2005**, *127*, 7511.
(21) McEnaney, B.; Mays, J.; Chen, X. *Fuel* **1998**, *77*, 557.
(22) Ravikovitch, P. I.; Vishnyakov, A.; Russo, R.; Neimark, A. V. *Langmuir* **2000**, *16*, 2311.
(23) Bhatia, S. K.; Tran, K.; Nguyen, T. X.; Nicholson, D. *Langmuir* **2004**, *26*, 9612.

(24) Do, D. D. *Adsorption Analysis: Equilibria and Kinetics*; Imperial College Press: London, 1998.
(25) Steele, W. A. *The Interaction of Gases with Solid Surfaces*; Pergamon Press: Oxford, U.K., 1974.
(26) Kowalczyk, P.; Holyst, R.; Terzyk, A. P.; Gauden, P. A. *Langmuir* **2006**, *22*, 1970.
(27) Frenkel, D.; Smit, B. *Understanding Molecular Simulation Form Algorithms To Applications*; Academic Press: London, 1996.
(28) Allen, M. P.; Tildesley, D. J. *Computer Simulation of Liquids*; Clarendon: Oxford, U.K., 1987.
(29) Widom, B. *J. Chem. Phys.* **1963**, *39*, 2808.
(30) Dell, R. M.; Rand, D. A. J. *Clean Energy*; The Royal Society of Chemistry: Cambridge, U.K., 2004.
(31) Kaneko, K.; Cracknell, R. F.; Nicholson, D. *Langmuir* **1994**, *10*, 4606.
(32) Matranga, K. R.; Myers, A. L.; Glandt, D. *Chem. Eng. Sci.* **1992**, *47*, 1569.